Desalination and Water Treatment
www.deswater.com

doi: 10.5004/dwt.2020.26262

204 (2020) 388–399
November

Fabrication and characterization of low cost electro-spun carbon fibers from organosolv bagasse lignin: effect of modification conditions

Khadiga Mohamed Abas[a], Amina Abdel Meguid Attia[a,*], Ahmed Ali Ahmed Nada[b], Mona Abdel Hamid Shouman[a], Maged Shafik Antonious[c]

[a]*Laboratory of Surface Chemistry and Catalysis, National Research Center, 33 El-Bohouth St., Dokki, P.O. Box: 12622, Giza, Egypt, Tel. +01006563002; email: amina_abdelmeguid@yahoo.com (A.A.M. Attia), Tel. +01022197965; email: mohamedkhadiga728@yahoo.com (K.M. Abas), Tel. +01270097332; email: monashouman@yahoo.com (M.A.H. Shouman)*
[b]*Pretreatment and Finishing of Cellulose Based Textiles Department, National Research Center, Giza, Egypt, Tel. +01147798440; email: ahmed_nada@hotmail.com (A.A.A. Nada)*
[c]*Department of Chemistry, Faculty of Science, Ain-Shams University, Cairo, Egypt, Tel. +01225607846; email: antonious_maged@hotmail.com (M.S. Antonious)*

Received 27 January 2020; Accepted 13 June 2020

ABSTRACT

Sugarcane bagasse is an agro-residues product of the sugarcane industry and owing to its plentiful accessibility; it has broadly studied for lignocellulosic conversion to the production of value-added commercial products. In this context, organosolv delignification of bagasse was executed employing acetic and formic acid along with dilute H_2SO_4 as a promoter at 100°C. Organosolv bagasse lignin (OBL) blended with renewable resource-based cellulose acetate (CA) at different ratios. Electrospinning technique has been issued for fabricating lignin nanofibers. Iodine treatment of nanofibers was inspected to assist the thermostabilization handling. The nanofibers were successfully converted into carbon fibers (CFs) through oxidative thermal stabilization in the air at 220°C and subsequently carbonized at 600°C. The investigated samples were identified with scanning electron microscopy, Fourier transform infrared analysis, thermal gravimetric analysis, and N_2 (77 K) adsorption. Tensile properties (stress, strain, young`s modulus) of electrospun nanofibers were greatly ameliorated via deposition of polyaniline (m-toluidine) through the formation of (OBL/CA/P-mTol) composite via *in-situ* oxidative chemical polymerization technique. This study extends the potential applicability of composite for water purification and stipulates a promising approach to MB dye removal of aqueous solutions.

Keywords: Bagasse lignin; Organosolv bagasse lignin (OBL); Carbon fibers (CFs); Conducting polymer (poly aniline: m-toluidine)

1. Introduction

Environmental subjects like global warming as well as the consumption of natural resources had increased interests in concerning our dependence on fossil fuel as a source of energy and materials [1]. The industry of lignocellulosic biomass permitted green possible alternatives to fossil resources in order to enable the increasing trend of world's demand for petroleum usage [2]. Recovery of low-cost lignocellulosic materials to products of superior characteristics exists a feasible chance of improvement on energy security and greenhouse emissions reduction. Lignocellulosic resources contain agricultural residues (corn crops, wheat rice, sugarcane bagasse, and empty fruit bunches, etc.), forest residues, energy crops, and food wastes. The annual production of sugarcane in Egypt is about 16 million tons/y.

* Corresponding author.

After harvest, sugarcane was treated to extract the sugar and molasses components. Bagasse is the fibrous residue that is sustained after sugarcane stalks are squished to extract their juice. Currently, 85% of bagasse production is burnt, and there is an excess of bagasse which is deposited in empty fields changing the landscape [3]. Bagasse is selected as a pattern of raw material in manufacturing new products due to its low fabrication cost and high-quality green end material. It consists of 50% cellulose and 25% each of hemicellulose and lignin. Additionally, it also provides numerous advantages in comparison to other crop residues and can be respected as a rich solar energy reservoir because of its low ash content, high yields, and annual regeneration capability [4]. The use of natural fiber (bagasse) in combination with polymers is conducted to achieve some degree of reinforcement of the fibers to the polymer. This has been done in most of the published cases of the literature. However, the interest in the usage of natural fibers in bio-composites goes over their advantages for developing new and mechanically improved substances [5].

Carbon fibers (CFs) are materials of great technological and industrial importance because of their extraordinary chemical, magnetic, electrical, and mechanical characteristics. The main raw material for producing CFs is polyacrylonitrile (PAN) which is a synthetic petroleum-based polymer. Other types of CFs are derived from petroleum pitch, coal, and rayon [6]. According to the precursor material applied, the properties of the CFs differ from each other. The CFs synthesize process includes spinning, oxidative stabilization at 180°C–250°C with low heating rate, and carbonization under inert gas at 1,000°C to yield CFs. In some proceedings, this approach is not efficient, but it can be enhanced by pre-treating the fibers. Iodine has been conducted as a process to intensify the thermal treatment process of several materials during the carbonization process [7]. Furthermore, it is famed to form charge transfer complexes about electron-rich molecules like those with lone pairs and aromatic rings in the shape of polyiodides [8].

Electrospinning is considered a suitable technique for producing CFs precursors to the potential for commercial applicability. Numerous studies have been previously illustrated that nanofibers from electrospinning demonstrate many unique characteristics, like large surface areas, high porosity, and superior mechanical performance [9]. A straightforward method of adjusting electrospinnability is to blend lignin with high molecular weight polymer additives like polyvinyl alcohol (PVA) [10], polyethylene oxide (PEO) [11], PAN and cellulose acetate (CA) [12,13]. CA is the most utilized derivative of cellulose, and widely used in filtrations (such as reverse osmosis and ultra-filtration) and in biomedical implementation for its biocompatibility [12,13]. Cellulose, acetic acid, and acetic anhydride are combined together to form CA. This process is neutralized by the addition of a small amount of sulfuric acid. CA has weak intra-molecular hydrogen bonds and solvents applied for it in common which are simple such as acetone, N,N-dimethylformamide (DMF), tetrahydrofuran (THF), etc. The effect of acetone can be alleviated using acetone/DMF solvent to produce stable nanofiber morphology and persistent nano-fiber of diameters between 110 nm and 1.5 μm [14].

The high cost of PAN as a precursor consuming petroleum resources aroused researchers to search for alternative fiber precursors to synthesize cheaper and environmentally friendly CFs. Recently, a broad range of renewable resource-based materials has been studied for the synthesis of carbon materials. Foremost among them, lignin has been seemed a promising candidate as a precursor for carbon materials. It is considered the second largest carbon reservoir after carbohydrate [15]. The biosphere contains about 30% of organic carbon and 40% of the energy in biomass [16], and is the only natural polymer formed of aromatics. The usage of lignin is greatly under-developed owing to its complexity and recalcitrance [17]. Currently, over 50 million tons of lignin are produced annually by the pulp and paper industry around the world, over 96% of it is addressed as a waste by-product and burnt for heat [18]. The isolated lignin has a mutinous structure of low purity; this has impeded the recovery of lignin into low molecular weight aromatic compounds. Thus, the advancement to an efficient process of lignin de-polymerization is significant from both scientific and economic prospects.

One of the most predominant strategies for lignin isolation is organosolv pre-treatment, which provides sulfur-free lignin with high purity, and makes it a suitable precursor of various applications. The characteristics of organosolv lignin are greatly dependent on the biomass substrate and on the organosolv pre-treatment technique. In many cases, further de-polymerization brings to low selectivity among yields, which are ascribed to the re-condensation of lignin during isolation. Several researches have focused on the improvement in organosolv lignin conversion. This depends on the inhibition of lignin re-condensation and reaching an efficient reaction system [19,20]. The presence of acids as a catalyst creates acid-catalyzed degradation of the monosaccharide into furfural and 5-hydroxymethyl furfural, then condensation reactions arise between lignin and these reactive aldehydes [21].

Over the last decade, different matrix polymers had been developed in order to eliminate poor mechanical properties from renewable resources (lignin) and provide renewable composites better in electrical and thermal conductive properties. Conducting polymers have been explored for their potential petition for many applications, like antistatic coatings, biosensors, and energy storage devices. Amongst these polymers, polyaniline (PANI) is regarded as one of the most versatile conducting polymers due to its excellent chemical stability, high electronic conductivity, relevant low cost of the monomer, ease of synthesis, and tunable properties. Thus, PANI is a good prospect of coating natural fibers to meet the requirements of current disposable technology concerning electrically conductivity, electro-activity, lightweight, and flexibility. PANI coated natural fibers such as mango, jute, and coconut fibers have established their properties in many fields [22].

Adsorption is referred to the presence of a higher concentration of a particular substance, either solid or liquid, at the surface comparatively to its bulk form medium. The adsorption processes incite as a result of molecular physical bonds between the adsorbate and the adsorbent [23]. The bond between the adsorbate and adsorbent will be strengthened by designing higher surface area of the

adsorbent or depleting the contact time among them. Surface modification also improved the interaction between adsorbate and adsorbent [24]. Polymeric substances are feasible as an adsorbent composite with respect to their rigidity, adjustable surface chemistry, and good selectivity toward organic adsorbate [25]. Their efficiency is depending on the degree of chemical activation, nature, and extent of functionality grafted on the polymeric surface.

The main contribution of this work is the delignification of bagasse using a mixture of organic solvents (formic acid/acetic acid) in presence of sulfuric acid as a catalyst. The extracted lignin has been successfully electro-spun through blending with CA with different ratios as an electro-spun polymer. The obtained fiber mats were thermo-stabilized, then carbonized at 600°C producing CFs (carbon fibers). By *in-situ* oxidative chemical polymerization, OBL/CA (0.5:1) nanofibers are modified by the PANI using m-toluidine as a monomer, HCl as a dopant and ammonium peroxydisulfate $(NH_4)_2S_2O_8$ as an oxidant to produce OBL/CA/P-mTol fibers composite which ameliorated the mechanical properties. Scanning electron microscopy (SEM), Fourier transform infrared spectroscopy (FTIR), thermo-gravimetric analysis (TGA), and N_2 (77 K) measurements were also carried out to characterize the investigated samples. Additionally, the mechanical characteristics including stress, strain, and strength of the produced fibers and fibers/polymer composite have been investigated; also the removal of methylene blue dye (MB) was studied.

2. Materials and methods

Bagasse (B) feedstock was collected from rural surroundings in Egypt. Prior to its processing, the raw material was washed under tap water several times followed by washing with double distilled H_2O. After thorough washing, the bagasse was cut into small pieces and dried under sunlight for 5 d to remove all the moisture content. Subsequently, the dried bagasse pieces were washed with hot water and dried in an oven at 90°C for 24 h. The oven dried bagasse was ground and sieved under 50 mesh screens, and then the lignocellulosic biomass was submitted to the extraction process.

Organic solvents for pretreatment of bagasse; formic acid (85%), acetic acid (85%), and sulfuric acid (H_2SO_4) (98%) were obtained from Sigma-Aldrich (United States). CA (average Mn = ~30 kDa) polymer was obtained from Fisher-Scientific (United Kingdom). Solvents for blending polymers; acetone and dimethyl formamide (DMF) were purchased from Sigma-Aldrich. Chemicals for bio-fiber modification; hydrochloric acid (HCl), ammonium peroxydisulfate ($(NH_4)_2S_2O_8$) (APS), and iodine crystals were purchased from Fisher-Scientific (Waltham, MA). All previous chemicals were used without applying any post-treatment. The monomer solution of aniline (m-toluidine) was obtained from Merck. Before utilizing, it was distilled under a vaccum and stored in the dark at 15°C. Methylene blue dye (MB) was obtained from RIEDEL-DE HAEN AG.

2.1. Organosolv fractionation

Delignification process was submitted in a closed reflux system containing 10 g of dry bagasse precursors of an organosolv mixture of formic acid:acetic acid [70:30 (v/v) ratio]. Liquid–solid ratios were maintained at 10:1 (v/wt). The experiment was performed at 100°C under atmospheric pressure for 2 h. Sulfuric acid was added as a catalyst 0.2% (v/v) for the lignin/reagent mixture. After cooking, the spent cooking liquor was filtered out and washed with water continuously. Organosolv bagasse lignin (OBL) was precipitated from the spent black liquor by adding five folds of distilled water and settled at room temperature for 1 h, subsequently the precipitated lignin was filtered through a buchner funnel and washed several times of distilled water, then the purified lignin was dried in a vacuum oven at 90°C. Fig. 1 illustrates the detailed delignification steps of bagasse precursor.

2.2. Chemical characterization of extracted lignin

2.2.1. Ash content

The ash content was determined gravimetrically using TAPPT test method.T-413. A constant weight of moisture free OBL was placed in a porcelain crucible and calcined in a muffle furnace at a regulated temperature range at 525°C ± 25°C for 4 h. Then, lignin sample was set in a desiccator for 1 h prior to weighing [26]. This procedure was conducted in triplicate until constant weight. The ash content was determined by the following equation:

$$\text{Ash content}\left(\%\right)=\left(A/B\right)\times 100 \quad (1)$$

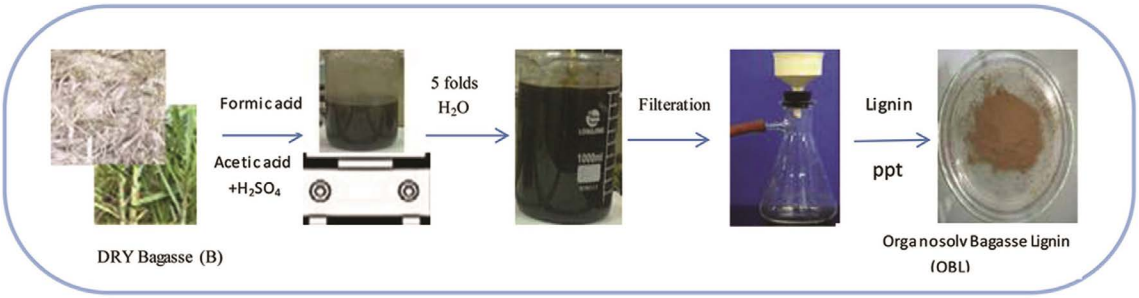

Fig. 1. Procedure of organosolv process.

where *A* is the weight of ash (g), and *B* is the weight of the dried lignin samples (g).

2.2.2. Moisture content

Moisture content was assessed using the standard official methods of analysis of the Association of Official Analytical Chemist (1990). This included drying the sample to a constant weight at 100°C and calculating moisture content as the loss in weight of the dried samples [27] by applying the following equation:

$$\text{Moisture content}\ (\%) = \left(\frac{C-B}{C}\right)\times 100 \tag{2}$$

where *C* is the weight of moist Lignin (g), and *B* is the weight of dry lignin (g).

2.2.3. Dry matter content

The material remaining after water elimination is referred to as dry matter content. In this study, it was determined by drying the sample (OBL) in an oven at 60°C for 8 h until a constant weight [27]. The percentage of dry matter was calculated from the following equation:

$$\text{Dry content}\ (\%) = \left(\frac{B}{C}\right)\times 100 \tag{3}$$

where *B* is the weight of dry lignin (g) and *C* is the weight of moist lignin (g).

2.2.4. Empirical formula

The molecular formula for the extracted lignin sample (OBL) was determined by C, H, and O percentages resulted from elemental analysis [28]. All the above chemical characteristics are tabulated in Table 1.

2.3. Electro-spinning process

A weighed amount of (CA) was dissolved in a mixture of acetone and DMF in a ratio of (2:1) according to the previous published work [29] to obtain a CA solution at a concentration of 12% (wt/v). OBL was dissolved in DMF (5.5% (wt/v), then blended with CA solution in different ratios (0.1:1, 0.5:1, and 0.75:1 v/v) in an acetone/DMF mixture. The total polymer concentrations of (12.6%, 13.8%, and 14.4% (wt/v)), respectively, were retained across the three ratios. These solutions were electrospun under fixed electrical potential of 22.5 kV across distance of 15 cm between the needle nozzle and the collector. The feed rate of the solutions was controlled at 0.5 mL/h as revealed in Fig. 2. Electrospinning process was carried out at room temperature [30].

2.4. Iodine-treatment of fibers

The OBL/CA fibers were placed into a ceramic boat, and then inserted into a sealed glass jar containing iodine crystals. The iodine jar was inserted into an air oven at 100°C for 15 min. Afterwards, the jar was cooled to room temperature, later fibers were detached [13]. The as-received nanofibers OBL/CA (0.5:1) was selected for all the proceeding experiments in this study.

2.5. Thermo-stabilization and carbonization treatment

The as-spun fiber mats, iodine treated and non-treated (OBL/CA fibers), were mounted on a metal rack inside a muffle furnace and pointed to oxidative stabilization at heating rate 1°C/min from room temperature to 180°C and

Table 1
Physicochemical characterization for OBL

Specifications	Content %
Ash content	0.1
Moisture content	4
Dry content	96
C	59
O	5.9
H	35
Empirical formula	$C_9H_{10.7}O_4$

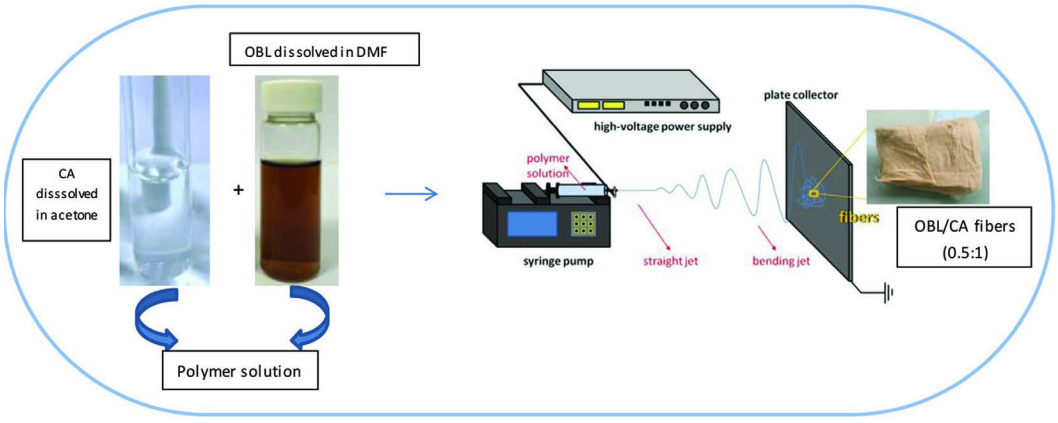

Fig. 2. Photograph of polymer solution through electro-spinning apparatus.

220°C under an air atmosphere for 1 h. The iodine-treated samples were fused at these temperatures.

Thus, the stabilized fiber mat (non-iodinated OBL/CA) was placed in a porcelain crucible and carbonized in a tubular furnace. During carbonization, the stabilized fibers were heated from room temperature to 600°C at 3°C/min, then retained isothermally for 15 min. N_2 was applied to flow rate 0.5 standard cubic feet per hour to maintain an inert atmosphere.

2.6. Composite fabrication

OBL/CA fibers mat (0.25 g) was dispersed in 25 mL of (0.4 M) APS (oxidant) by sonication for half an hour. Polymerization was initiated by drop-wise addition of (0.1 M) m-toluidine (monomer) and (0.1 M) HCl (dopant) to aforementioned solution through sonication for another 1 h. The weight ratio of fibers:monomer (0.5:1) was kept constant in 50 mL total reaction solution [31,32]. The poly(m-toluidine) coated OBL fiber mat composite [OBL/CA/P-mTol] was then filtered and washed with distilled water to remove oligomers and non-treated monomers, then dried in an air oven at 70°C.

2.7. Characterization

Characterization of the examined samples supplies important information related to the stability, composition, and functionality. The images of the samples were acquired by SEM using SEM-JEOL (JXA-840A Electron Probe Micro-Analyzer, Japan). The elemental analysis was carried out by using a carbon, hydrogen, and nitrogen (CHN) analyzer (automatic Vario Micro-analyzer System). Functional group chemistry was performed by using FTIR spectroscopy (FTIR-6100 Jasco spectrophotometer) in transmission modes. The specific surface area, total pore volume, and average pore diameters of the samples were determined by N_2 adsorption–desorption isotherms measured at 77 K using (Quanta Chrome NOVA automated gas sorption system version 1.12). The TGA of the samples was done in flowing N_2 gas (200 mL/min at a heating rate of 5°/min from 25°C to 900°C using (Perkin Elmer 7 series thermal analysis).

The investigation into the adsorption properties of the obtained tested samples with respect to methylene blue dye (50 mg/L) was conducted to 10 mg of adsorbents (CFs, OBL/CA (0.5:1) and OBL/CA/P-mTol fiber mats) in 10 mL flask at pH = 6.5 without any external adjustment [33]. Each sample was kept in a rotary shaker at 180 rpm for 24 h at ambient temperature to reach equilibrium. The adsorbents were separated from aqueous solutions. The absorbance of the supernatant was detected using Shimadzu UV-vis spectrophotometer (type UV-2401PC) at 664 nm.

The amount of adsorption at equilibrium (q_e (mg/g)) was calculated using the following equation:

$$q_e = \left(C_0 - C_e\right) \cdot \frac{V}{m} \tag{4}$$

where C_0 and C_e (mg/L) are the initial and equilibrium liquid phase concentrations, V (L) is the volume of the equilibrium solution, and m (g) is the mass of the adsorbent.

The removal efficiency (R %) of adsorbents was detected by:

$$R(\%) = \frac{\left(C_0 - C_e\right)}{C_0} \times 100 \tag{5}$$

where R is the percentage removal of the dye.

2.8. Mechanical analysis

Tensile tests were performed on the as-spun OBL/CA and its modified composite fiber mats by uniaxial tensile testing employing a universal (LR10K; L1oyd Instruments, Fareham, UK). The capacity of the load cell used was 5 N. The tensile testing of tested samples was carried out in a humid environment for 5 d. Tensile speed was 2 mm/min. An epoxy adhesive was used to adhere the fiber mats (30 mm length × 10 mm width × 0.2 mm thickness) to a paper mounting tabs with gauge length 20 mm. The strain rate was 0.2 mm/min. Tensile tests began once the sample was securely gripped and cut away both sides of the tab. Tensile stress and strain of the investigated samples were calculated by applying the following equations:

$$\sigma = \frac{F}{A} \tag{6}$$

where σ is the stress (N/mm^2 or MPa), F is the load (N), and A is the cross-sectional area (mm^2).

$$\varepsilon = \frac{\left(L - L_0\right)}{L_0} \tag{7}$$

where ε is the strain, L_0 is the actual length sample (mm), L is the sample length at break point (mm).

Young's modulus, E, is the measure of the ability of a material to tolerate changes in length under lengthwise tension or compression. It can be displayed through the linear regression analysis of the initial linear portion of the stress-strain curves by applying the formula represented as follows:

$$E = \frac{\text{Stress}}{\text{Strain}} = \frac{\Delta\sigma}{\Delta\varepsilon} \tag{8}$$

where E is young's modulus (MPa) and tensile strength can be determined from the maximum stress point (σ_{max}, MPa).

3. Result and discussion

3.1. Electro-spun fiber morphology

The diameters of electrospun beads-free fibers from three different selected fiber mats of OBL/CA were investigated via SEM micrographs. The results are depicted in Fig. 3. The SEM image of OBL, Fig. 3a, shows surface morphology like cauliflower with diameter (80 ± 30 nm). Different polymer ratios were tested to discover the best ratio to create smooth fibers without beads. Figs. 3b and c display that samples of ratios (0.1:1) and (0.5:1) generated

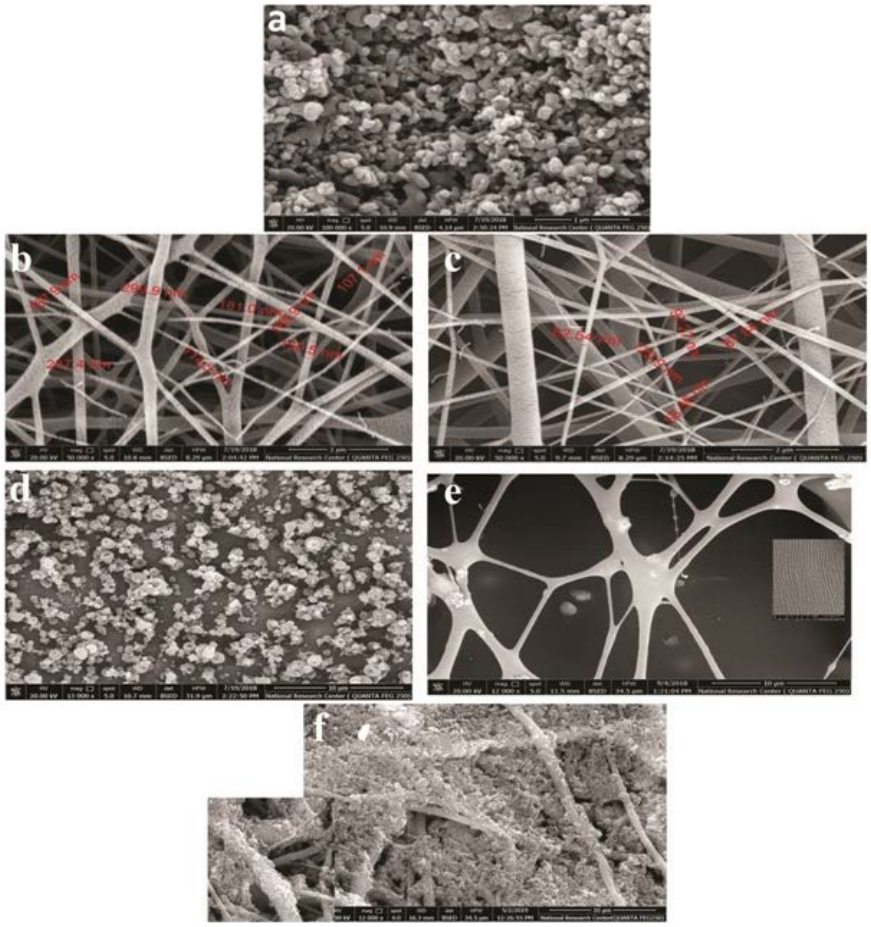

Fig. 3. SEM morphology of the fabricated; (a) OBL, (b) OBL:CA (0.1:1), (c) 0.5:1, (d) 0.7:1, (e) CFs, and (f) OBL/CA/P-mTol fiber composite.

a dense network nanofibers. The fibers diameters did not differ significantly between both samples, both of them being close to 200–230 ± 150 nm. The sample of (0.75:1) ratio, Fig. 3d has not frame electrospun nanofibers, they shaped assembled features of beads instead of fibers. This can be attributed to the strong interaction between polyphenolic cross-linked lignin with CA, which probably effects on the polymer solution viscosity which led to weak spinnability [10,34,35].

The SEM micrograph of OBL/CA (0.5:1) fibers mats with poly(m-toluidine), (fiber diameter; 487 ± 200 nm) Fig. 3f comprised poly(m-toluidine) as continues layers on the fiber mat surface in the form of agglomerates. This feature may be aroused to be a prerequisite good adsorbent [36].

The effect of iodine absorption on thermal treatment of OBL/CA (0.5:1) was investigated. Iodination promotes the lignin powder to maintain its shape during thermal treatment (Fig. 4). As evidence, the fiber mats turned rapidly into deep brown in color owing to the enhancement of lignin aromatic structure [13]. Then, it was stabilized at two different temperatures (180°C and 220°C), as a result the fibers mats were melt and fused. Therefore, iodination doesn't recuperate the thermostabilization process and has no impact on the preservation of the fiber morphology which is not influenced by temperature.

Consequently, non-iodinated OBL/CA fibers mats of ratio (0.5:1) (v/v) were thermally stabilized at 220°C, then carbonized at 600°C producing carbon fibers with diameters range (267 ± 199) nm as appeared in Fig. 3e.

3.2. FTIR spectroscopy

FTIR spectra of OBL, CA, and CFs are demonstrated in Fig. 5a, moreover as-spun OBL/CA fibers and its polymer composite are submitted in Fig. 5b, respectively. The variation in spectra demonstrates that the functional groups of OBL were changed to some extent after electro-spinning and carbonization. The FTIR bands assignments to Fig. 5a are indexed in Table 2.

A comparison of the spectra displays that all the investigated samples have common peaks at frequencies (3,430; 2,930; 2,850; and 1,740–1,714 cm^{-1}). The broad characteristic band of 3,430 cm^{-1} is assigned to (–OH) hydroxyl stretching vibration. The intensity of this band was weakened significantly in the produced CFs due to the formation of hydrogen bonds between CA and lignin [37]. Also, the process of dehydration [38] and hydroxylation eventuated [39] throughout the carbonization process. Furthermore, the evolution of water contents [40]. Besides, the increase in the intensity of peaks at 2,930 and 2,850 cm^{-1}

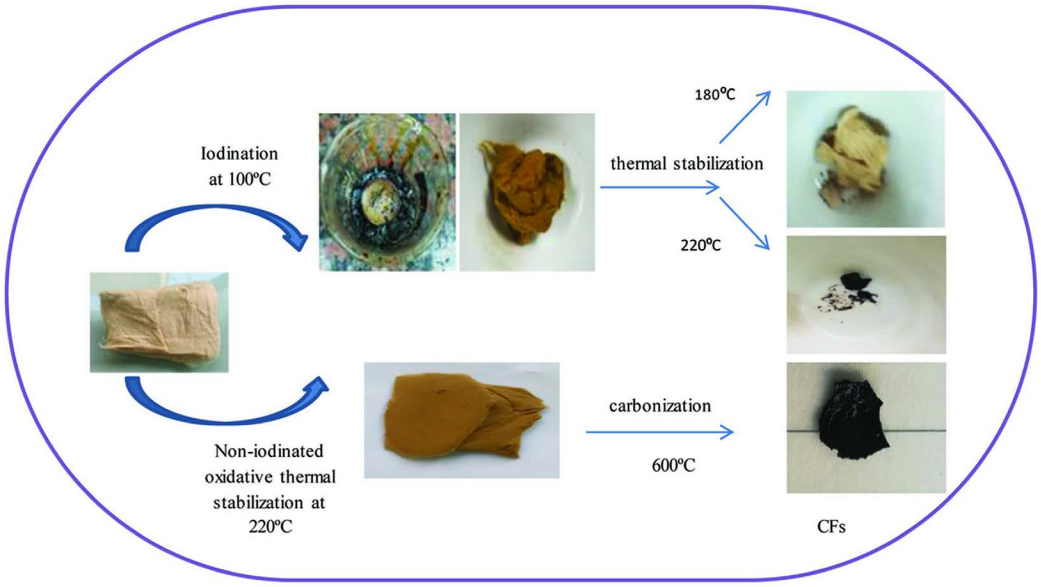

Fig. 4. Optical images of iodinated and non-iodinated fibers after thermal treatment.

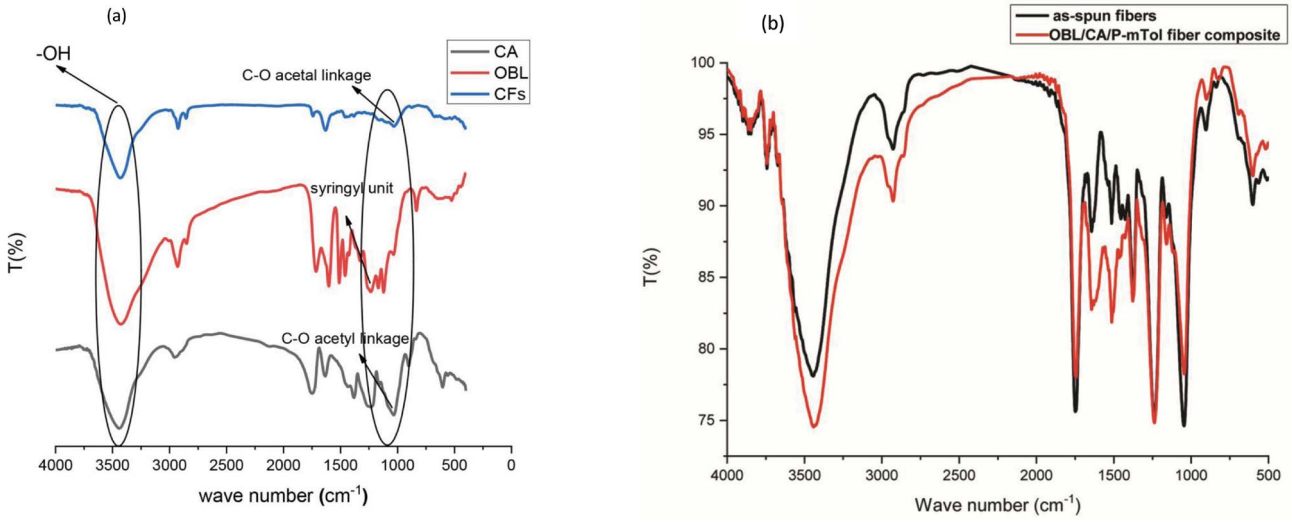

Fig. 5. (a) FT-IR spectra of; CA, OBL, and CFs and (b) FT-IR spectra of; As-spun fiber and its polymer composite.

was observed corresponding to C–H vibrations of methyl and methylene groups. The band frequency at a range of 1,740–1,714 cm^{-1} is assigned to C=O stretching from unconjugated carbonyl ketones [41].

The region between 1,381; 1,234; and 1,032 cm^{-1} provides information about structural units of CA. The signal placed at 1,381 cm^{-1} can be ascribed to bending vibrations of C–CH_3 present in the methyl group [42,43]. Peaks observed between 1,234 and 1,032 cm^{-1} are characteristic of materials based on cellulose and they can be linked to the carboxylate group. They are characterized as alkoxy stretching to ester group (C–O–C) and acetal linkage of cellulose backbone [37] which appears clearly in the functionality of the produced CFs as a small broad peak with lower intensity.

Lignin powders depict typical lignin absorption bands of frequencies (1,459; 1,328; 1,234; and 1,168 cm^{-1}) assigned to (–OCH_3) methoxy group, –OH phenolic, C–O stretching of syringyl unit and stretching vibration of ether bond formation [41], respectively. These bands indicate the presence of phenyl propanoid group due to aromatic skeletal vibration. The presence of phenyl propanoid structures is responsible for the transformation of lignin to polycyclic building blocks throughout carbonization which is a suitable feature of carbon precursor [41]. Moreover, the absorption band frequency of 1,602–1,511 cm^{-1} is represented to C–H of the aromatic ring skeleton of OBL that appears in the produced CFs accompanied by slight shifting observed at 1,631 cm^{-1}.

The FTIR spectra of as-spun fibers and polymer composite are viewed in Fig. 5b, respectively. The characteristic transition of fiber mats at 3,000–3,500, 1,750–1,100, and 700–900 cm^{-1} appeared in the spectra of both samples (as-spun fiber and composite). The intensity of the broad

Table.2
FTIR interpretation of the tested samples

Assignment	Wave number (cm^{-1})		
	CA	OBL	CFs
–OH	3,443	3,426	3,430
C–H stretching	2,955	2,929	2,925
		2,850	2,855
C=O stretching	1,748	1,714	1,742
C–H aromatic skeleton		1,602	1,631
		1,511	1,457
$C–OCH_3$		1,459	
$C–CH_3$	1,381		
–OH phenolic		1,328	
C–O stretching of ester in C.A and syringyl unit in O.B.L	1,234	1,234	
C–O acetyl linkage	1,032		1,030
Ether band formation		1,168	

characteristic band increased in the composite spectrum owing to the combination of stretching vibration of N–H and C–H group resulted from m-toluidine polymer with O–H hydroxyl group and C–H around 3,400 and 3,000 cm^{-1}, respectively. Two extra sharp bands observed at 1,644 and 1,513 cm^{-1} in the polymer composite spectrum are characteristic to C=C and C=N in quinoid and benzene ring of P-mTol [44]. The band at 1,280 cm^{-1} corresponds to C–N stretching vibration. This implies that as-spun fibers are complete coated with poly(m-toluidine).

3.3. Thermal analysis

The TGA thermo-grams and the first derivative of thermo-gravimetric analysis (DTG) of OBL and CFs are shown in Figs. 6a and b, respectively. Table 3 summarizes the thermal parameters for the investigated samples.

The initial degradation for OBL sample begun below 100°C with weight loss of (4.8%) is appertaining to the weight loss of water. The degradation process is moderate between 100°C and 200°C and a plateau can be observed. The second degradation stage around 100°C–400°C accompanied with significant mass loss of (48%) portrays the main degradation process of lignin. Degradation of the complex structure of OBL in this temperature district concerned fragmentation of inter-unit linkage between phenolic hydroxyl, carbonyl groups, and benzylic hydroxyl, liberating monomeric phenols into the vapor phase besides some residual hemicellulose contents that are connected to the lignin structure. All of these factors may accelerate the degradation process. The syringyl units are constructed into the lignin macromolecule mainly by ether bonds. The ether bonds between syringyl units are simpler to scission [45]. DTG_{max} for OBL appeared in the range of 361°C. These data may explain the highest thermal stability of OBL sample. Above 400°C, the degradation process of OBL sample is possibly relevant to the slow decomposition of some aromatic rings in lignin. Above 850°C, most of all lignin samples still maintain un-volatilized owing to

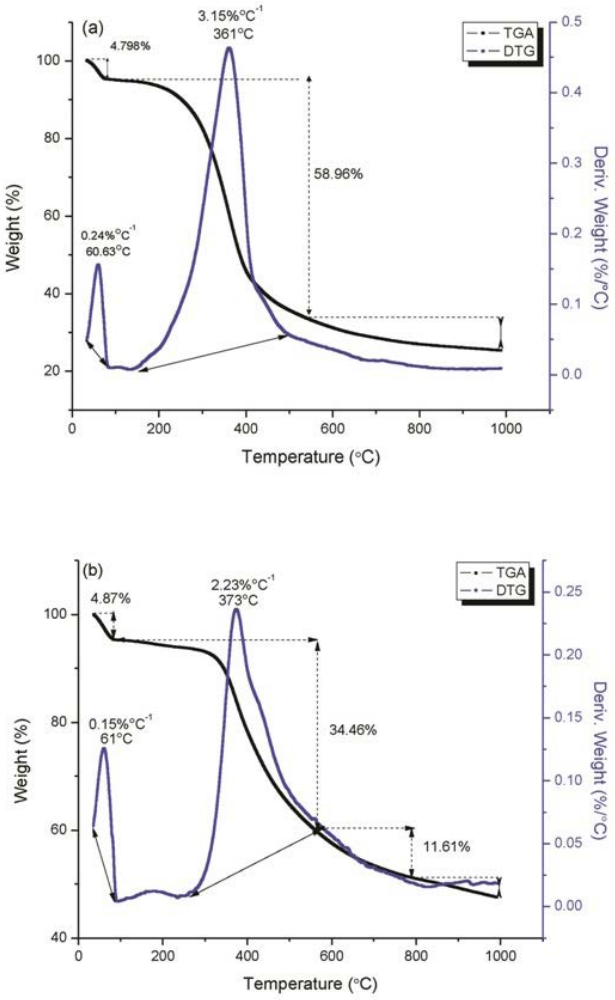

Fig. 6. TGA/DTG spectra of; (a) OBL and (b) CFs.

the formation of highly condensed aromatic structures [46] causing in general weight loss of (10.8%) [47].

CFs manifested good thermal stability as compared to OBL sample having 49% residual weight as compared to the 36% for OBL at 1,000°C (Table 3). The weight loss noticed mainly below 95°C may be due to the vaporization of moisture absorbed on the surfaces of CFs. The weight loss from 95°C to 550°C (34.5%) might be related to the unstable oxygen-containing groups existing in the CFs [48]. There is an immediate decrease in the weight (11.6%) at a temperature around 550°C that is returned to the removal of more stable oxygen functionalities (including fragmentation of inter-unit linkage, releasing of monomers, derivatives of phenols, and degradation of aromatic rings into vapor) [49], or due to the incomplete carbonization of the fibers. The maximum weight loss rate of CFs degradation steps at temperature (61°C and 373°C) are (0.15% and 2.23%), respectively.

3.4. Surface area and adsorption analysis of MB

The specific surface area (S_{BET}, m^2/g), total pore volume (V_t, cc/g), and average pore diameter (D_p, nm) of OBL/CA fiber mat, CFs, and OBL/CA/P-mTol fiber mat composite are

Table.3
Thermal parameters of OBL and CFs

Sample	Stage I		Stage II and III		Yield %
	Interval (°C)	DTG_{max} (°C)	Interval (°C)	DTG_{max} (°C)	
OBL	35–100	60.6	100–400 400–600	361	36.4
CFs	40–100	61	100–550 550–800	373	49

summarized in Table 4. All samples were fabricated from the same precursors, however, exhibit different textural properties.

It is noteworthy that the OBL/CA fiber mat (37.4 m^2/g) shows a significant change in S_{BET} after carbonization (577 m^2/g). During carbonization, dehydration, and degradation as well as aligomeric products are formed from transfiguration, thus resulting in a carbon framework with large porosity. This leads to the production of ordered mesoporous carbon structures [50]. The specific surface area (252 m^2/g), pore volume (1.22 cc/g), and average pore diameters (1.94 nm) of composite sample manifested the inhibitory effect of poly(m-toluidine) on the mat nanofiber assembly. Moreover, its deficiency in graphitic crystallinity, topological defects, and structural disorder of modified composite was considered to facilitate the generation of internal pores accompanied increasing with specific surface area [51] compared to its neat OBL/CA fiber mat (37.4 m^2/g). These results correlate to those attained through SEM and FTIR.

The adsorption mechanism depends on the surface of adsorbent and the structure of the dye molecule. Upon dissolving MB dye in water, its molecules dissociate into MB^+ and Cl^-. The presence of hydroxyl and phenol groups on the surface of lignin fiber mat can interact with MB dye. This response has proven adsorption behavior with adsorption capacity of (25 mg/g). For poly(m-toluidine), the adsorption occurs mainly on imino, amino, and benzene ring structure. Since MB is a planar aromatic molecule and poly(m-toluidine) has a lot of aromatic π–π staking thus hydrophobic interaction could arise between poly(m-toluidine) and MB through H-bonding [52], whilst the adsorption of cationic MB onto the basic sites of poly(m-toluidine) occurs via electrostatic interaction [53,54] with adsorption capacity of (29 mg/g). Thereby we predicate a synergetic phenomenon between OBL and poly(m-toluidine) [55]. Comparison of MB dye uptake in this study with various materials from literature was recorded in Table 5.

Table 4
Surface texture properties of the produced samples

Surface textural characteristics	OBL/CA fiber mat	CFs	OBL/CA/P-mTol fiber mat composite
S_{BET} (m^2/g)	37.4	577	252
V_t (cc/g)	0.5	0.2	1.22
D_p (nm)	50	1.7	1.94
Q_e (mg/g)	25	17.8	29
R (%)	51.6	35.6	56.4

Table 5
Comparison of MB dye uptake with other materials reported in the literature

Adsorbent	Q_e (mg/g)	References
OBL/CA fiber mat	25	This work
CFs	17.8	This work
OBL/CA/P-mTol fiber mat composite	29	This work
Bagasse	49.8–56.5	[56]
MWCNTs	60	[31]
PANI	19.7	[57]
MWCNTs/P-NMA nanocomposite	29.4	[31]
MWCNT-magnetic composite	11.86	[58]

3.5. Mechanical performance

The results of the mechanical tests are outlined in Table 6 and typical stress–strain curves of electrospun nanofibers (OBL/CA) and OBL/CA/P-mTol composite are illustrated in Fig. 7. It can be noted that strength, stress, and strain at break increased for polymer composite compared to as-spun fibers with minor decrease in young's modulus (6.7 MPa). The presence of strong interactions between fibers and poly(m-toluidine) as stated by FTIR and SEM explains the presence of tensile strength, stress, and strain at break. The overall yield strength and ultimate tensile strength of the resulting composite were improved from 0.2 to 0.9 and 0.3 to 1.1 MPa, respectively. The same tendency was observed for stress and strain at break which increased from 0.3 to 0.9 MPa and from 25% to 34%, respectively.

The interfacial adhesion between the fibers and polymer matrix plays a vital role in strengthening the mechanical behavior of fiber mats-reinforced composite. The results of this study demonstrate that when a load is employed to as-spun nanofibers and its composite oriented in the direction of uniaxial force, they are stretched. Fig. 7 displays that two notable phases occurred. The first phase includes the fiber straighten and reorienting through the direction of the utilized load with no fiber breakage. The second phase represents the fiber fracture and slippage until it reaches maximum stress.

The decrease in mechanical strength of as-spun OBL/CA fibers before modification with aniline polymers (poly (m-toluidine)) is ascribed to their porous flabby structure

Table.6
Mechanical properties (strength, young's modulus, strain, and stress at break) of electrospun fiber mat and its polymer composite

Specimen	Strength (MPa)		Young's modulus (MPa)	Strain at break (%)	Stress at break (MPa)
	Yield strength (Y)	Ultimate tensile strength (UT)			
As-spun OBL/CA fibers	0.2	0.3	10	25	0.3
OBL/CA/P-mTol fiber composite	0.9	1.1	6.7	34	0.9

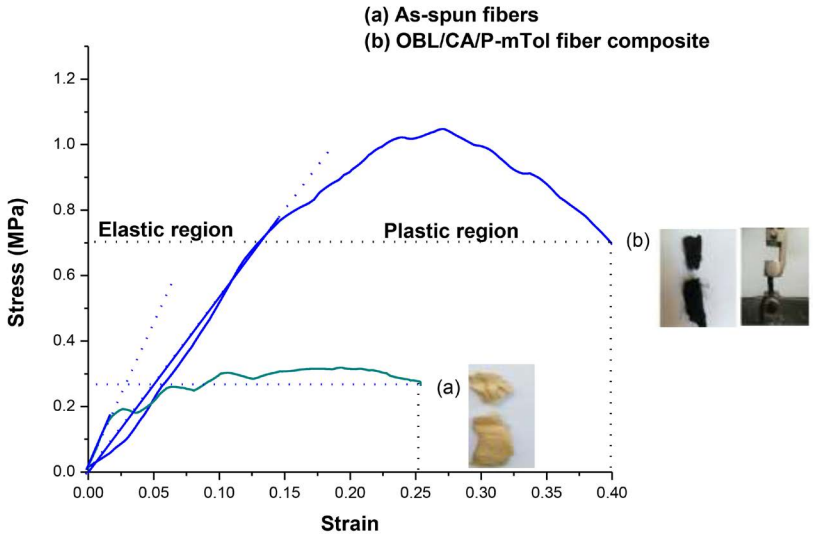

Fig. 7. Stress-Strain relationship of; (a) As-spun OBL/CA fibers and (b) OBL/CA/P-mTol fibers composite.

Table.7
Comparison between tensile properties of the produced electrospun fiber mats with various research work

Specimen	Tensile strength (MPa)	Young's modulus (MPa)	Reference
As-spun OBL/CA fibers	0.3	10	This work
As-spun OBL/CA/P-mTol fiber composite	1.1	6.7	This work
PCL/lignin nanocomposite	0.99 ± 0.05	0.16	[63]
CA/PANI	3 ± 1	34 ± 7	[59]
PCL fibers		5	[64]
PVDF		6.5 ± 0.4	[36]
PVDF/PANI		6.9 ± 0.3	[36]

due to a poor adhesion force between the fibers. Accordingly, failures of the fiber–fiber interface arise and the absence of chemical cross-linking point in cellulose fibers generates low mechanical strength [59]. Moreover, the lack of strength of lignin is derived from the limitation of its molecular orientation owing to its amorphous cross-linked structure [60].

Modification of the as-spun nanofibers affords interfacial interaction between the polymer matrix and dispersed fiber filler. This permits an effective π-conjugation length of linear derivative aniline polymers from C=C and C=N through the quinoid structure as appeared from FTIR spectra [61]. The hydrophobic character and aromaticity in lignin facilitate the interaction with hydrophobic poly(m-toluidine). Blending of OBL with an emeraldine base of aniline polymers exhibited a good homogeneous blend, which facilitates the interaction between amine groups of (aniline) with carbonyl group and hydroxyl groups of (lignin) [62]. A summary of some researchers devoted their studies to fabricate electrospun nanofibers-reinforced composites are highlighted in Table 7.

4. Conclusion

The objective of this study is to extract lignin from bagasse by organosolv treatment employing (formic acid and acetic acid) in presence of sulfuric acid as a catalyst

producing OBL. Electrospun nanofibers were successfully generated from blends of OBL and cellulose acetate of different ratios by the electrospinning process. Iodine handling led to the fusion of fibers throughout the thermostabilization step. The relative ratio of (0.5:1) (OBL/CA) possessed the best fiber morphology along with bead-free fibers with small diameters distribution. Spun nanofibers were transformed into carbon fibers (CFs) utilizing carbonization temperature up to 600°C. Coating as-spun nanofibers by poly(m-toluidine)via *in-situ* oxidative chemical polymerization endow a significant improvement in the mechanical properties. This composite showed up a good adsorption capability of (29 mg/g) for MB dye removal in comparison to the other fabricated samples.

References

[1] P.A. Owusu, S. Asumadu-Sarkodie, A review of renewable energy sources, sustainability issues and climate change mitigation: civil and environmental engineering, Cogent Eng., 3 (2016) 1–14.

[2] H.V. Lee, S.B.A. Hamid, S.K. Zain, Conversion of lignocellulosic biomass to nanocellulose: structure and chemical process, Sci. World J., 2014 (2014) 1–21.

[3] T.C. Mokhena, M.J. Mochane, T.E. Motaung, L.Z. Linganiso, O.M. Thekisoe, S.P. Songca, Sugarcane Bagasse and Cellulose Polymer Composites, in: Sugarcane - Technol. Res., 3rd ed., chapter 12, IntechOpen., 2018, pp. 225–240, doi:10.5772/intechopen.71497.

[4] A. Balaji, B. Karthikeyan, C.S. Raj, Bagasse fiber–the future biocomposite material: a review, Int. J. Chem. Tech. Res., 7 (2015) 223–233.

[5] T. Gurunathan, S. Mohanty, S.K. Nayak, A review of the recent developments in biocomposites based on natural fibres and their application perspectives, Composites, Part A, 77 (2015) 1–25.

[6] X. Huang, Fabrication and properties of carbon fibers, Materials, 2 (2009) 2369–2403.

[7] S. Rom, J. Libra, N. Berge, E. Sabio, K. Ro, L. Li, B. Ledesma, S. Bae, Hydrothermal carbonization: modeling, final properties design and applications: a review silvia, Energies, 11 (2018) 1–28.

[8] E. Powell, Y. Lee, R. Partch, D. Dennis, T. Morey, Pi–Pi complexation of bupivacaine and analogues with aromatic receptors: implications for overdose remediation, Int. J. Nanomed., 2 (2007) 449–459.

[9] A. Greiner, S. Agarwal, J.H. Wendorff, A. Greiner, Use of electrospinning technique for biomedical applications, Polymer, 49 (2008) 5603–5621.

[10] M. Ago, K. Okajima, J.E. Jakes, S. Park, O.J. Rojas, Lignin-based electrospun nanofibers reinforced with cellulose nanocrystals, Biomacromolecules, 13 (2012) 918–926.

[11] V. Poursorkhabi, A.K. Mohanty, M. Misra, Electrospinning of aqueous lignin/poly(ethylene oxide) complexes, Appl. Polym. Sci., 132 (2015) 1–9.

[12] A. Oroumei, B. Fox, M. Naebe, Thermal and rheological characteristics of biobased carbon fiber precursor derived from low molecular weight organosolv lignin, ACS Sustainable Chem. Eng., 3 (2015) 758–769.

[13] M. Schreiber, S. Vivekanandhan, A.K. Mohanty, M. Misra, Iodine treatment of lignin-cellulose acetate electrospun fibers: enhancement of green fiber carbonization, ACS Sustainable Chem. Eng., 3 (2015) 33–41.

[14] C. Liu, K. Lai, W. Liu, R. Sun, Preparation of carbon nanofibres through electrospinning and thermal treatment, Polym. Int., 58 (2009) 1341–1349.

[15] B.M. Upton, A.M. Kasko, Strategies for the conversion of lignin to high-value polymeric materials: review and perspective, Chem. Rev., 116 (2018) 2275–2306.

[16] C. Li, X. Zhao, A. Wang, G.W. Huber, T. Zhang, Catalytic transformation of lignin for the production of chemicals and fuels, Chem. Rev., 115 (2015) 11559–11624.

[17] I. Cesarino, P. Araújo, A.P. Domingues, P. Mazzafera, An overview of lignin metabolism and its effect on biomass recalcitrance, Braz. J. Bot., 35 (2012) 303–311.

[18] F. Cotana, G. Cavalaglio, A. Nicolini, M. Gelosia, A. Petrozzi, L. Brinchi, Lignin as co-product of second generation bioethanol production from ligno-cellulosic biomass, Energy Procedia, 45 (2014) 52–60.

[19] J.S. Luterbacher, A. Azarpira, A.H. Motagamwala, F. Lu, J. Ralph, J.A. Dumesic, Lignin monomer production integrated into the c-valerolactone sugar platform, Energy Environ. Sci., 8 (2015) 2657–2663.

[20] K. Barta, G.R. Warner, E.S. Beach, P.T. Anastas, Depolymerization of organosolv lignin to aromatic compounds over Cu-doped porous metal oxides, Green Chem., 16 (2014) 191–196.

[21] J. Esteban, P. Yustos, M. Ladero, Catalytic processes from biomass-derived hexoses and pentoses: a recent literature overview, Catalysts, 8 (2018) 1–39.

[22] A. Mirabedini, J. Foroughi, G.G. Wallace, Developments in conducting polymer fibres: from established spinning methods toward advanced applications, RSC Adv., 6 (2016) 44687–44716.

[23] N. Yuan, H. Cai, T. Liu, Q. Huang, X. Zhang, Adsorptive removal of methylene blue from aqueous solution using coal fly ash-derived mesoporous silica material, Adsorpt. Sci. Technol., 37 (2019) 333–348.

[24] A. Dabrowski, Adsorption-from theory to practice, Adv. Colloid Interface Sci., 93 (2001) 135–224.

[25] J.A. Laksmono, M. Sudibandriyo, A.H. Saputra, A. Haryono, Development of porous structured polyvinyl alcohol/zeolite/carbon composites as adsorbent, IOP Conf. Ser.: Mater. Sci. Eng., 201 (2017) 1–6.

[26] J. Sameni, S. Krigstin, D. dos Santos Rosa, A. Leao, M. Sain, Thermal characteristics of lignin residue from industrial processes, BioResources, 9 (2014) 725–737.

[27] M.F. Zainuddin, R. Shamsudin, M.N. Mokhtar, D. Ismail, Physicochemical properties of pineapple plant waste fibers from the leaves and stems of different varieties, BioResources, 9 (2014) 5311–5324.

[28] M.A. Rahandi, A. Rizkia, L. Risanto, L. Hakim, Isolation and characterization of lignin from alkaline pretreatment black liquor of oil palm empty fruit bunch and sugarcane bagasse, MEV J., 3 (2012) 1–5.

[29] A.A. Nada, R.A. Abdelazeem, A.H. Elghandour, N.Y. Abou-Zeid, Protection of conjugated linoleic acid into hydrophobic/hydrophilic electrospun fibers, J. Drug Delivery Sci. Technol., 44 (2018) 482–490.

[30] A.A. Attia, M.S. Antonious, M.A. Shouman, A.A. Nada, K.M. Abas, Processing and fundamental characterization of carbon fibers and cellulose nanocrystals derived from bagasse, Carbon Lett., 29 (2019) 145–154.

[31] S.M. Sayyah, A. Attia, N. Fathy, M. Shouman, A. Khaliel, K. Abas, Fabrication, characterization and adsorption studies of carbon nanotubes synthesis from camphor reinforced with poly N-methyl aniline, Int. J. Adv. Res., 3 (2015) 1084–1095.

[32] A.A. Attia, M.A. Shouman, S.M. Sayyah, N.A. Fathy, A.B. Khaliel, K.M. Abas, Sequestration of methylene blue and lead ions by MWCNT modified with polyconducting polymers, Egypt. J. Chem., 60 (2017) 221–241.

[33] E. A, N. Laouedj, B. Ahmed, Effect of pH solution on the optical properties of cationic dyes in dye/maghnia montmorillonite suspensions, J. Chem. Eng. Process Technol., 2 (2011) 1–6.

[34] H. Fong, I. Chun, D.H. Reneker, Beaded nanofibers formed during electrospinning, Polymer, 40 (1999) 4585–4592.

[35] N. Bhardwaj, S.C. Kundu, Electrospinning: a fascinating fiber fabrication technique, Biotechnol. Adv., 28 (2010) 325–347.

[36] C. Merlini, G.M. de Oliveira Barra, S.D.A. da Silva Ramôa, G. Contri, R. dos Santos Almeida, M.A. d'Ávila, B.G. Soares, Electrically conductive polyaniline-coated electrospun poly(vinylidene fluoride) mats, Front Mater., 2 (2015) 1–6, doi: 10.3389/fmats.2015.00014.

[37] K. Rodríguez, J. Sundberg, P. Gatenholm, S. Renneckar, Electrospun nanofibrous cellulose scaffolds with controlled microarchitecture, Carbohydr. Polym., 100 (2014) 143–149.

[38] A. Funke, F. Ziegler, Hydrothermal carbonization of biomass: a summary and discussion of chemical mecha- nisms for process engineering, Biofuels, Bioprod. Biorefin., 4 (2010) 160–177.
[39] D.S. Ross, B.H. Loo, D.S. Tse, A.S. Hirschon, Hydrothermal treatment and the oxygen functionalities in Wyodak coal, Fuel., 70 (1991) 289–295.
[40] X. Ma, C. Yuan, X. Liu, Mechanical, microstructure and surface characterizations of carbon fibers prepared from cellulose after liquefying and curing, Materials, 7 (2014) 75–84.
[41] A. Mandal, D. Chakrabarty, Isolation of nanocellulose from waste sugarcane bagasse (SCB) and its characterization, Carbohydr. Polym., 86 (2011) 1291–1299.
[42] H. Liu, Y.L. Hsieh, Ultrafine fibrous cellulose membranes from electrospinning of cellulose acetate, J. Polym. Sci., Part B: Polym. Phys., 40 (2002) 2119–2129.
[43] Z. Ma, S. Ramakrishna, Electrospun regenerated cellulose nanofiber affinity membrane functionalized with protein A/G for IgG purification, J. Membr. Sci., 319 (2008) 23–28.
[44] S. Quillard, G. Louarn, S. Lefrant, A.G. Macdiarmid, Vibrational analysis of polyaniline: a comparative study of leucoemeraldine, emeraldine, and pernigraniline bases, Phys. Rev. B: Condens. Mater., 50 (1994) 12496–12508.
[45] B.E. Khaldi-Hansen, M. Schulze, B. Kamm, Qualitative and Quantitative Analysis of Lignins from Different Sources and Isolation Methods for an Application as a Biobased Chemical Resource and Polymeric Material, S. Vaz Jr., Ed., Analytical Techniques and Methods for Biomass, Springer International Publishing, Switzerland, 2016, pp. 1–280.
[46] J.L. Wen, B.L. Xue, S.L. Sun, R.C. Sun, Quantitative structural characterization and thermal properties of birch lignins after auto-catalyzed organosolv pretreatment and enzymatic hydrolysis, J. Chem. Technol. Biotechnol., 88 (2013) 1663–1671.
[47] A. Alzagameem, B.E. Khaldi-Hansen, D. Büchner, M. Larkins, B. Kamm, S. Witzleben, M. Schulze, Lignocellulosic biomass as source for lignin-based environmentally benign antioxidants, Molecules, 23 (2018) 1–25.
[48] X.Z. Tang, B. Yu, R.V. Hansen, X. Chen, X. Hu, J. Yang, Grafting low contents of branched polyethylenimine onto carbon fibers to effectively improve their interfacial shear strength with an epoxy matrix, Adv. Mater. Interfaces, 2 (2015) 1–7.
[49] T.A. Khan, A. Gupta, S.S. Jamari, R. Jose, M. Nasir, A. Kumar, Synthesis and characterization of carbon fibers and their application in wood composites, BioResources, 8 (2013) 4171–4184.
[50] M. Oschatz, R. Walczak, Crucial factors for the application of functional nanoporous carbon-based materials in energy and environmental applications, C. J. Carbon Res., 4 (2018) 1–22, doi: 10.3390/c4040056.
[51] Z. Li, H. Zhang, Q. Liu, L. Sun, L. Stanciu, J. Xie, Fabrication of high-surface-area graphene/polyaniline nanocomposites and their application in supercapacitors, ACS Appl. Mater. Interfaces, 5 (2013) 2685–2691.
[52] M.A. Al-Ghouti, J. Li, Y. Salamh, N. Al-laqtah, G. Walker, M.N.M. Ahmad, Adsorption mechanisms of removing heavy metals and dyes from aqueous solution using date pits solid adsorbent, J. Hazard. Mater., 176 (2010) 510–520.
[53] A.P. Mathew, Z. Karim, M. Grahn, J. Mouzon, M.K. Oksman, Nanoporous membranes with cellulose nanocrystals as functional entity in chitosan: removal of dyes from water, Carbohydr. Polym., 112 (2014) 668–676.
[54] C. Kaewprasit, E. Hequet, N. Abidi, J.P. Gourlot, Application of methylene blue adsorption to cotton fiber specific surface area measurement: part I. Methodology, J. Cotton Sci., 2 (1998) 164–173.
[55] A.H. Norzilah, A. Fakhru'L-Razi, T.S.Y. Choong, A.L. Chuah, Surface modification effects on CNTs adsorption of methylene blue and phenol, J. Nanomater., 2011 (2011) 1–18.
[56] L.W. Low, T.T. Teng, A. Ahmad, N. Morad, Y.S. Wong, A novel pretreatment method of lignocellulosic material as adsorbent and kinetic study of dye waste adsorption, Water Air Soil Pollut., 218 (2011) 293–306.
[57] M. Maruthapandi, V.B. Kumar, J.H.T. Luong, A. Gedanken, Kinetics, isotherm, and thermodynamic studies of methylene blue adsorption on polyaniline and polypyrrole macro-nanoparticles synthesized by C-dot-initiated polymerization, ACS Omega, 3 (2018) 7196–7203.
[58] J.L. Gong, B. Wang, G.M. Zeng, C.P. Yang, C.G. Niu, Q.Y. Niu, W.J. Zhou, Y. Liang, Removal of cationic dyes from aqueous solution using magnetic multi-wall carbon nanotube nanocomposite as adsorbent, J. Hazard. Mater., 164 (2009) 1517–1522.
[59] A.C. Baptista, I. Ropio, B. Romba, J.P. Nobre, C. Henriques, J.C. Silva, J.I. Martins, J.P. Borges, I. Ferreira, Cellulose-based electrospun fibers functionalized with polypyrrole and polyaniline for fully organic batteries, J. Mater. Chem. A, 6 (2018) 256–265.
[60] V. Davé, A. Prasad, H. Marand, W.G. Glasser, Molecular organization of lignin during carbonization, Polymer, 34 (1993) 3144–3154.
[61] Y. Kaitsuka, N. Hayashi, T. Shimokawa, E. Togawa, H. Goto, Synthesis of polyaniline (PANI) in nano-reaction field of cellulose nanofiber (CNF), and carbonization, Polymers, 8 (2016) 1–12.
[62] P.C. Rodrigues, M. Muraro, C.M. Garcia, G.P. Souza, M. Abbate, W.H. Schreiner, M.A.B. Gomes, Polyaniline/lignin blends: thermal analysis and XPS, Eur. Polym. J., 37 (2001) 2217–2223.
[63] M.A. Salami, F. Kaveian, M. Rafienia, S. Saber-Samandari, A. Khandan, M. Naeimi, Electrospun polycaprolactone/lignin-based nanocomposite as a novel tissue scaffold for biomedical applications, J. Med. Signals Sens., 7 (2017) 228–238.
[64] M. Kancheva, A. Toncheva, N. Manolova, I. Rashkov, Enhancing the mechanical properties of electrospun polyester mats by heat treatment, Express Polym. Lett., 9 (2015) 49–65.